

# Di-muon Analysis Using CMS Open Data

A report submitted in partial fulfillment of the requirements for  
*the award of the degree of*

**Master of Science in Physics**

by

**Mallam Eswar  
(22PGPHY25)**



CENTRAL UNIVERSITY OF KARNATAKA

**Department of Physics  
School Of Physical Sciences  
Central University Of Karnataka**

**Submitted on: July 10, 2024**

**Supervisor**

Dr. Jyothsna Rani Komaragiri

Assistant Professor

Indian Institute of Science, Bangalore.

# Declaration

I hereby certify that the work, which is being presented in the project report, entitled **Dimuon Analysis Using CMS Open Data**, in partial fulfillment of the requirement for the award of the Degree of Master of Science in Physics and submitted to the institution is an authentic record of my own work carried out during the period **01/02/2024 to 10/07/2024** under the supervision of **Dr. Jyothsna Rani Komaragiri**.

I also cited the reference about the text(s)/figure(s)/table(s)/equation(s) from where they have been taken.

The matter presented in this report has not been submitted elsewhere for the award of any other degree or diploma from any institutions.

Date: \_\_\_\_\_

Signature of the Candidate

# CERTIFICATE

This is to certify that the work entitled “**Di-muon Analysis Using CMS Open Data**” is the bonafide work carried out by **Mr. MALLAM ESWAR**. The student registration number is **2022PGPHY25** of academic year 2022-2024, M.Sc. Physics, Department of Physics, School of Physical Sciences, Central University of Karnataka, Kalaburagi. This work is supervised under the guidance of Dr.Jyothsna Rani Komaragiri as a partial fulfilment of requirements for the award of Master’s Degree in Physics.

Signature of  
Head of the Department

Signature of  
Project Supervisor

Signature of  
In home mentor

# Acknowledgements

I would like to express my sincere gratitude to

My supervisor, Professor Dr. Jyothsna Rani Komaragiri, whose guidance and expertise were invaluable throughout this project.

Dr. Suchismitha Sahoo, In home mentor at Campus CUK, for providing the opportunity to work with Dr. Jyothsna Rani Komaragiri and for supporting me throughout this project with insightful discussions that enriched this study.

The CMS experiment team, for the open data recorded in 2012 during Run B and C, which provided the essential data and resources crucial to this project.

Dr. Bharat Kumar, Head of the Department of Physics, and the Dean of Physical Sciences, for allowing me to conduct this project outside the campus at IISc and The professors at CUK for their academic support, which was invaluable throughout various stages of this work.

I am also thankful to everyone who supported me throughout this project.

# Abstract

This project focuses on analyzing the dimuon spectrum using open data from the CMS experiment at the CERN Large Hadron Collider (LHC), recorded in 2012. The Compact Muon Solenoid (CMS) is a general-purpose detector designed to investigate a wide range of physics phenomena, including the search for new particles predicted by the Standard Model and its extensions. The dimuon spectrum provides a powerful tool for studying particle resonances, given the precise measurements of muons that CMS is capable of.

In this analysis, we examine a range of particle resonances observed in the dimuon spectrum, starting from the  $\eta$  meson and extending to the Z boson. The properties of these particles, including their invariant mass, transverse momentum, pseudorapidity, and azimuthal angle ( $\phi$ ), are meticulously analyzed to gain deeper insights into their behavior and characteristics.

Moreover, the CMS experiment is pivotal in the search for Supersymmetry (SUSY) particles, which may decay into leptons, including muons. SUSY is a theoretical extension of the Standard Model that proposes a symmetry between fermions and bosons.

By leveraging the comprehensive dataset from the CMS experiment and employing advanced analysis techniques, this project aims to contribute to the understanding of particle properties and the ongoing search for new particles, including those predicted by Supersymmetry.

# Contents

<b>Declaration</b>	<b>1</b>
<b>Acknowledgements</b>	<b>3</b>
<b>Abstract</b>	<b>4</b>
<b>1 Introduction</b>	<b>8</b>
1.1 The Standard Model and Particle Physics . . . . .	8
1.1.1 Particles in the Standard Model . . . . .	11
1.1.2 Fermions . . . . .	11
1.1.3 Bosons . . . . .	12
<b>2 Experimental Overview</b>	<b>14</b>
2.0.1 Design of the Large Hadron Collider (LHC) . . . . .	15
2.1 Compact Muon Solenoid (CMS) detector . . . . .	15
2.1.1 CMS Detector . . . . .	15
2.1.2 CMS Detector Design . . . . .	16
2.1.3 The Tracking System . . . . .	17
2.1.4 The Electromagnetic Calorimeter . . . . .	17
2.1.5 The Hadronic Calorimeter . . . . .	17
2.1.6 The Magnet System . . . . .	18
2.1.7 The Muon Chambers . . . . .	18
2.2 Trigger and Data Acquisition System . . . . .	20
<b>3 Dimuon Analysis in Particle Physics</b>	<b>21</b>
3.0.1 Introduction . . . . .	21
3.0.2 Particle Production in High-Energy Collisions . . . . .	21
3.0.3 Dimuon Production Mechanisms . . . . .	21
3.0.4 Experimental Setup and Data Analysis . . . . .	21
3.0.5 Discovery and Characterization of New Particles . . . . .	21
3.1 Indirect detection of particles . . . . .	22
3.2 ROOT for Analysis . . . . .	25
<b>4 The Dimuon Spectrum</b>	<b>28</b>
4.1 Meson Resonance Fits . . . . .	29
4.1.1 Eta Particle $\eta$ Resonance Fit . . . . .	29
4.1.2 Omega Particle Resonance Fit . . . . .	30
4.1.3 Phi Particle $\phi$ Resonance Fit . . . . .	31
4.1.4 J/Psi Particle $J/\psi$ Resonance Fit . . . . .	32
4.1.5 Psi Prime $\psi'$ Resonance Fit . . . . .	33

4.1.6	Upsilon $Y(1S)$ Resonance Fit . . . . .	34
4.1.7	Z Boson Resonance Fit . . . . .	35
<b>5</b>	<b>Kinematics</b>	<b>36</b>
5.1	Coordinate Systems . . . . .	38
5.2	Kinematic plots of the particle Resonances . . . . .	39
<b>6</b>	<b>Conclusion and Future Work</b>	<b>43</b>
	<b>References</b>	<b>43</b>

# List of Figures

1.1	Standard Model of Particle Physics (credits: CERN ) . . . . .	9
2.1	The Compact Muon Solenoid (CMS) Detector(credits: CERN) . . . . .	16
2.2	Components of the CMS Detector . . . . .	19
2.3	Data acquisition system of CMS experiment . . . . .	20
3.1	The process where the Z boson decays to the muon and the antimuon . . . . .	22
3.2	Quantities $\eta$ , $\theta$ , and $\phi$ in the CMS detector . . . . .	24
4.1	Dimuon spectrum . . . . .	28
4.2	Eta Resonance Fit . . . . .	29
4.3	Omega Resonance Fit . . . . .	30
4.4	Phi Resonance Fit . . . . .	31
4.5	J/Psi Resonance Fit . . . . .	32
4.6	Psi Prime Resonance Fit . . . . .	33
4.7	Upsilon Resonance Fit . . . . .	34
4.8	Z Boson Resonance Fit . . . . .	35
5.1	Kinematic plot of j/psi . . . . .	41
5.2	Kinematic plot of psi prime . . . . .	42
5.3	Kinematic plot of Upsilon . . . . .	42
5.4	Kinematic plot of Z boson . . . . .	42

## CHAPTER 1

# Introduction

### 1.1 The Standard Model and Particle Physics

Galileo is known as being the first to use experiments to provide answers to the basic questions. Since then, we have learned how the universe functions, from tiny electrons to massive galaxies. We have searched for a single, universal theory to explain everything, and the standard model of particle physics—which describes the fundamental particles of which everything in the universe is composed has come the closest.

The Standard Model tells that everything in the universe is made of 12 matter particles (we will see what are these particles later in this chapter) interacting with three fundamental forces, with the Higgs boson playing a important role in giving mass to those particles. as you can see this model doesn't account for gravity, governed by Einstein's general relativity which deals with bigger objects , which remains challenging to integrate it into the tiny world of quantum framework.

Particles in the Standard Model Particles are divided into fermions, or matter particles, and bosons, or force carriers, in the standard model. All known matter is made up of fermions, which include electrons, up quarks, and down quarks. Another type of fermion is the neutrino, which is special because of its small mass and weak interactions. These particles exist in three generations, with four particles in each generation, for reasons that are still not completely understood. Higher generations exist, but they decay rapidly, with only the first generation producing stable matter.

The Higgs Boson 2012 saw the discovery of the Higgs boson, which interacts with the Higgs field to give other particles mass. Despite what the equations of the Standard Model seem to suggest, this interaction is essential to understanding why particles have mass.

The Standard Model explains how the twelve different kinds of matter particles that make up the universe interact with the three forces and are all connected together by a very unique particle known as the Higgs boson.

A few warnings before we begin. I said "three forces" first. However, the universe is governed by four fundamental forces. This indicates that there is an object missing from the image. That would be gravity, the most evident force at work in our surroundings but, paradoxically, the least understood. Indeed, we possess a highly successful theory of gravity. Albert Einstein gave it to us, and it's known as general relativity. However, the Standard Model does not include it for two valid reasons. The first is that the force

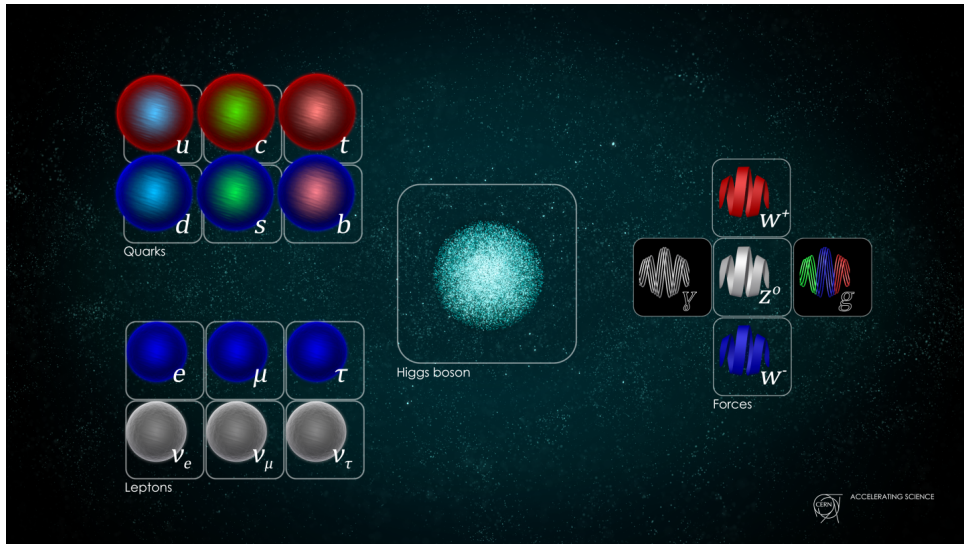


Figure 1.1: Standard Model of Particle Physics (credits: CERN )

of gravity is so tiny at the microscopic level that it hardly affects even one subatomic particle. The second is that we really don't know how to bring together the quantum world with the classical theory of general relativity. How one can look inside a black hole where quantum gravity effects are at play is a mystery to us.

The Standard Model is written in a language called quantum field theory, which presents a second warning. This indicates that matter is not essentially composed of particles at its most basic level. Rather, it is composed of fields, which are objects that resemble fluids and are dispersed throughout space. We refer to the intricate, harmonious dance these fields are performing to as the laws of physics. Particles that make up the physical world are the result of interactions between the fields. Using the language of particles makes understanding the Standard Model easier.

Many particles with a wide variety of names that can easily become confusing will be encountered as the Standard Model is assembled. However, one classification is by far the most significant: All particles are one of two types: force particles called bosons, or fermions, which are particles of matter. The quantum world is where fermions and bosons differ from one another. The Pauli exclusion principle is something that fermions have to abide by. I would say that this indicates that two fermions cannot be stacked on top of one another in space. These are the constituent parts of matter as a result. Bosons, on the other hand, are completely unrestricted by the Pauli exclusion principle, so they are free to measure on top of each other forever. The particles that mediate the forces are called bosons; we will discuss them in more detail later. Let's begin by examining the fermions for the time being.

There are only three matter particles that make up everything that exists: an electron and two types of quarks called up and down quarks. There are three quarks in each of the known proton and neutron. The neutron has two down quarks and an up quark, compared to the proton's two up quarks and one down. A collection of protons and neutrons is called a nucleus. An atom is created when you add electrons to the mixture. You are made of atoms put together in large quantities. This same set of three particles,

repeatedly rearranged in many different combinations, is the source of all the beauty and complexity we observe in the world.

### Neutrinos and Particle Generations

Neutrinos, the fourth class of matter particles, interact very weakly due to their small mass. For example, 100 trillion neutrinos pass through your body every second, most originating from the sun. Matter consists of four particles: electrons, up quarks, down quarks, and neutrinos. Intriguingly, nature created two more generations of these particles: the muon and tau, heavier counterparts to the electron, and charm, top, strange, and bottom quarks, heavier counterparts to up and down quarks. Additionally, there are tau and muon neutrinos. Higher-generation particles decay rapidly, leaving only the first generation stable.

### Bosons and Forces

The universe's forces are mediated by bosons: photons (electromagnetism), gluons (strong force), and W/Z bosons (weak force). Electromagnetic force affects electrically charged particles, with electric fields composed of photons. The strong force binds quarks in protons and neutrons via gluons, creating a confinement phenomenon where quarks can't exist independently. The weak force, responsible for particle decay, operates at subatomic distances.

### Mathematical Unity

A single equation, derived by Paul Dirac in the 1920s for the electron, applies to all particles, indicating a deep mathematical unity in the Standard Model. Despite understanding particle sets and forces, the reason for three generations of particles remains unclear. Forces give particles the ability to interact, making the universe dynamic and interesting.

We recently discovered that quarks are bound together by the strong force to form protons and neutrons, which make up the atomic nucleus. The amazing property of the weak force is that it can cause quarks to change their identities. An electron and neutrino are released when a down quark converts into an up quark, for instance. In other words, a neutron can change into a proton. We refer to this process as radioactive beta decay. In this sense, the nuclear fusion reactions which power the sun and generate the energy needed for life on Earth are caused by the weak force.

Lastly, the rapid decay of heavier matter particles into the three lighter and more stable fermions that comprise matter as we know it, such as the muon and strange quark, can be given to the weak force. Out of the three forces, only the weak force acts on every particle. It's the only force that neutrinos can feel, specifically. We refer to the particles connected to the weak force as the W and Z bosons. Now, let's finally meet the final element of the puzzle: the particle that, in many ways, connects the entire Standard Model.

The Higgs boson is this. I should point out to you first one startling fact before I explain why the Higgs boson is unique: there isn't a mass in any of the fundamental particles in the universe. It gets worse than that, though, because the Standard Model's equations prevent particles from having any mass at all! The photon and other massless

particles must move at the speed of light. Thus, why do massless matter particles not travel at the speed of light? This is the role of the Higgs boson. It plays a rather dramatic role in giving all fermions a mass. The Higgs field that governs the universe rather than the particle itself is the reason behind this.

### Higgs Field and the Standard Model

The Higgs field, akin to cosmic molasses, gives matter particles mass, with the Higgs boson confirmed in 2012 at CERN's Large Hadron Collider. The Standard Model consists of twelve matter particles interacting with the Higgs field and three forces. Despite its success, physicists believe there is more to discover. The Standard Model provides correct responses for almost all experiments, but we seek experiments where it fails to find new physics.

### Beyond the Standard Model

Questions remain about whether the three fundamental forces are separate or part of a Grand Unified Theory. Gravity, with its ripples in space-time known as gravitational waves, hints at quantum particles called gravitons, though detecting them is far off. The Standard Model also doesn't explain dark matter and dark energy, which constitute 95% of the universe's energy. Additional particles likely make up dark matter, potentially with their own forces and bosons.

### Unanswered Questions

Why are particles like the top quark much heavier than the electron, or neutrinos so light? These patterns suggest an underlying structure yet to be discovered. The goal is to uncover the next layer of reality, moving towards a theory of everything that explains the universe comprehensively, continuing Galileo's legacy of exploration.

## 1.1.1 Particles in the Standard Model

The Standard Model of particle physics is a comprehensive framework that describes the fundamental particles and forces that govern the universe, except for gravity. The particles in the Standard Model are divided into two main groups: fermions and bosons. Fermions are the building blocks of matter, while bosons are force carriers that mediate interactions between matter particles.

### 1.1.2 Fermions

Fermions are subdivided into quarks and leptons, each with six types, known as "flavors." These particles obey the Pauli exclusion principle, which means no two fermions can occupy the same quantum state simultaneously.

#### Quarks

Quarks are the fundamental constituents of protons and neutrons, which in turn make up the nuclei of atoms. They come in six flavors:

1. **Up (u)** and **Down (d)**: The lightest and most stable quarks. Protons are composed of two up quarks and one down quark, while neutrons consist of one up quark and two down quarks.

2. **Charm (c)** and **Strange (s)**: Heavier quarks that are produced in high-energy processes such as cosmic ray collisions or particle accelerator experiments.
3. **Top (t)** and **Bottom (b)**: The heaviest quarks. The top quark, in particular, has a mass close to that of a gold atom and exists only for a very short time before decaying into other particles.

Quarks are never found in isolation but are always confined within composite particles called hadrons (such as protons and neutrons) due to the "color" charge and the strong force.

## Leptons

Leptons do not experience the strong nuclear force. There are six leptons:

1. **Electron (e)**: The most familiar lepton, an essential component of atoms.
2. **Muon ( $\mu$ )** and **Tau ( $\tau$ )**: Heavier cousins of the electron. They are identical to the electron in charge and spin but have greater mass and decay rapidly.
3. **Neutrinos ( $\nu$ )**: Each charged lepton (electron, muon, tau) has a corresponding neutrino (electron neutrino  $\nu_e$ , muon neutrino  $\nu_\mu$ , and tau neutrino  $\nu_\tau$ ). Neutrinos are extremely light and neutral, making them incredibly difficult to detect as they rarely interact with matter.

### 1.1.3 Bosons

Bosons are particles that follow Bose-Einstein statistics and are responsible for carrying the forces of the Standard Model, except for gravity, which is not included in the model.

1. **Photon ( $\gamma$ )**: The carrier of the electromagnetic force, responsible for electric and magnetic interactions.
2. **W and Z Bosons**: These mediate the weak nuclear force, which is responsible for radioactive decay processes. The W boson carries a charge (either positive or negative), while the Z boson is neutral.
3. **Gluons ( $g$ )**: The force carriers for the strong nuclear force, which binds quarks together within protons, neutrons, and other hadrons. Gluons themselves carry the color charge and can interact with each other.
4. **Higgs Boson**: The Higgs boson is a scalar particle associated with the Higgs field, a universal field that gives mass to particles that interact with it. Its discovery at CERN in 2012 was a monumental achievement in particle physics.

These fermions and bosons together explain a vast array of physical phenomena, from the structure of atoms to the properties of nuclear reactions. However, the Standard Model is not the ultimate theory of everything; it doesn't include gravity (described by General Relativity), nor does it fully explain dark matter, dark energy, or the matter-antimatter asymmetry in the universe. Research continues in the quest to understand these mysteries, potentially leading to new physics beyond the Standard Model.

Table 1.1: Properties of Standard Particles

Particle	Symbol	Mass (GeV/ $c^2$ )	Charge ( $e$ )	Spin
Electron	$e^-$	$0.511 \times 10^{-3}$	-1	$\frac{1}{2}$
Electron Neutrino	$\nu_e$	$< 2 \times 10^{-9}$	0	$\frac{1}{2}$
Muon	$\mu^-$	0.106	-1	$\frac{1}{2}$
Muon Neutrino	$\nu_\mu$	$< 0.19$	0	$\frac{1}{2}$
Tau	$\tau^-$	1.777	-1	$\frac{1}{2}$
Tau Neutrino	$\nu_\tau$	$< 18.2$	0	$\frac{1}{2}$
Up Quark	$u$	0.0023	$+\frac{2}{3}$	$\frac{1}{2}$
Down Quark	$d$	0.0048	$-\frac{1}{3}$	$\frac{1}{2}$
Charm Quark	$c$	1.275	$+\frac{2}{3}$	$\frac{1}{2}$
Strange Quark	$s$	0.095	$-\frac{1}{3}$	$\frac{1}{2}$
Top Quark	$t$	173.21	$+\frac{2}{3}$	$\frac{1}{2}$
Bottom Quark	$b$	4.18	$-\frac{1}{3}$	$\frac{1}{2}$
Photon	$\gamma$	0	0	1
Gluon	$g$	0	0	1
Z Boson	$Z^0$	91.1876	0	1
W Boson	$W^\pm$	80.379	$\pm 1$	1

## CHAPTER 2

# Experimental Overview

The largest and most powerful hadron collider in the world, the Large Hadron Collider (LHC), is located at CERN, close to Geneva, Switzerland. The LHC aims to explore a new range of particle physics with an integrated luminosity of  $10^{34} \text{ cm}^{-2}\text{s}^{-1}$  and a center of mass energy of 14 TeV.

Nearly 10,000 scientists and engineers from various nations worked on the construction of this massive collider. Around 27 km in circumference, the LHC is located 574 feet below the Franco-Swiss border. When it reopened in 2021 after a three-year break for maintenance and upgrades, the center of mass energy of the two colliding beams was increased to 14 TeV from its previous value of 13 TeV.

A grid-based computer network [17] (representing 140 computing centres globally) is utilised for the analysis of LHC data. That grid, which links 36 nations worldwide, is the biggest computer grid in existence.

The largest and most powerful hadron collider in the world, the Large Hadron Collider (LHC), is located at CERN, close to Geneva, Switzerland. The LHC aims to explore a new range of particle physics with an integrated luminosity of  $10^{34} \text{ cm}^{-2}\text{s}^{-1}$  and a center of mass energy of 14 TeV.

Nearly 10,000 scientists and engineers from various nations worked on the construction of this massive collider. Around 27 km in circumference, the LHC is located 574 feet below the Franco-Swiss border. When it reopened in 2021 after a three-year break for maintenance and upgrades, the center of mass energy of the two colliding beams was increased to 14 TeV from its previous value of 13 TeV.

The LHC is anticipated to provide significant insights into the origins of the early universe, its structure, and the cause of particle masses. The primary objective of the LHC is to demonstrate the validity of the Standard Model by exploring the Higgs Boson. CERN made a formal announcement on July 4, 2012, regarding the discovery of a boson similar to the Higgs that supports the Standard Model. Verification of the super-symmetry theory, an extension of the Standard Model, is one of the LHC's other objectives. Additionally, as predicted by "String Theory," the LHC is built to detect extra dimensions [12].

Investigating the nature of "Dark Matter and Dark Energy" is another of the main objectives [1]. Moreover, the LHC is anticipated to provide some hints regarding "Grand Unified Theory" [2], which may be attained by fusing the strong and electroweak forces. Additionally, scientists want to know why the gravitational force is weak. The LHC is also looking for the nature of "Quark Gluon Plasma," which is assumed to have existed in the early universe, as well as the causes of the asymmetry between matter and anti-matter.

### 2.0.1 Design of the Large Hadron Collider (LHC)

Located under the Franco-Swiss border, an underground tunnel with a diameter of 1.3 meters was constructed between 1983 and 1988. Initially used by the "Large Electron Positron Collider (LEP)," this tunnel later housed the LHC, operational from 1988 to 2008.[16]

At the LHC, two proton beams collide at four interaction points. Beam focusing is assisted by numerous quadrupole magnets, while dipole magnets guide the beams along their circular path. The magnets are maintained at 1.9 K using liquid helium.

At a beam energy of 7 TeV, particle velocities approach  $0.999999991c$ . Protons reach this speed gradually, starting in the Linear Accelerator (LINAC) at 50 MeV, progressing through the Proton Synchrotron Booster (PSB) to 1.4 GeV, then the Proton Synchrotron (PS) to 26 GeV, and finally the Super Proton Synchrotron (SPS) to 450 GeV. The protons are then accelerated to 7 TeV in the main LHC ring.

The LHC features six detectors, including:

- CMS: A general-purpose detector focusing on the Higgs Boson and dark matter, among other inquiries.
- ATLAS: Another general-purpose detector aimed at exploring new physics, extra dimensions, and extensions of the standard model.
- ALICE: Dedicated to studying Quark Gluon Plasma and heavy ion collisions.
- LHCb: Specializes in b-physics and investigates matter-antimatter asymmetry.
- TOTEM and LHCf: Small, specialized detectors for specific research fields.

Each detector serves unique purposes in advancing our understanding of particle physics and cosmology.

## 2.1 Compact Muon Solenoid (CMS) detector

The Compact Muon Solenoid (CMS) detector, situated a hundred meters underground in the small agricultural commune of Cessy, France, is a monumental cylindrical onion of metal detectors (see Figure 2.1). It serves as one of two general-purpose detectors at the Large Hadron Collider (LHC), currently the world's largest particle collider. With a diameter spanning 15 meters and a length of 21 meters, the CMS detector is the second largest particle detector by volume. However, it holds the title of the heaviest detector in the world, weighing approximately fourteen thousand metric tonnes.

### 2.1.1 CMS Detector

The CMS detector, as its name implies, is made specifically by placing calorimeters inside a solenoid. The CMS detector has a total weight of 12,500 t, a length of 21.5 m, and a diameter of 16 m. In contrast, the ATLAS detector is

heavy in weight but not in size. The ATLAS detector has dimensions of 7,000 t, 46 m, and 25 m, respectively, for weight, length, and diameter. The configuration of both detectors is nearly symmetrical at the point where two beams interact. "Endcaps" surround the central barrel on both sides. The calorimeter, tracking detectors, and magnet coil are all located inside. The iron return yoke is interspersed with muon chambers. The CMS detector is shown schematically in Figure 2.1.

## CMS DETECTOR

Total weight : 14,000 tonnes  
Overall diameter : 15.0 m  
Overall length : 28.7 m  
Magnetic field : 3.8 T

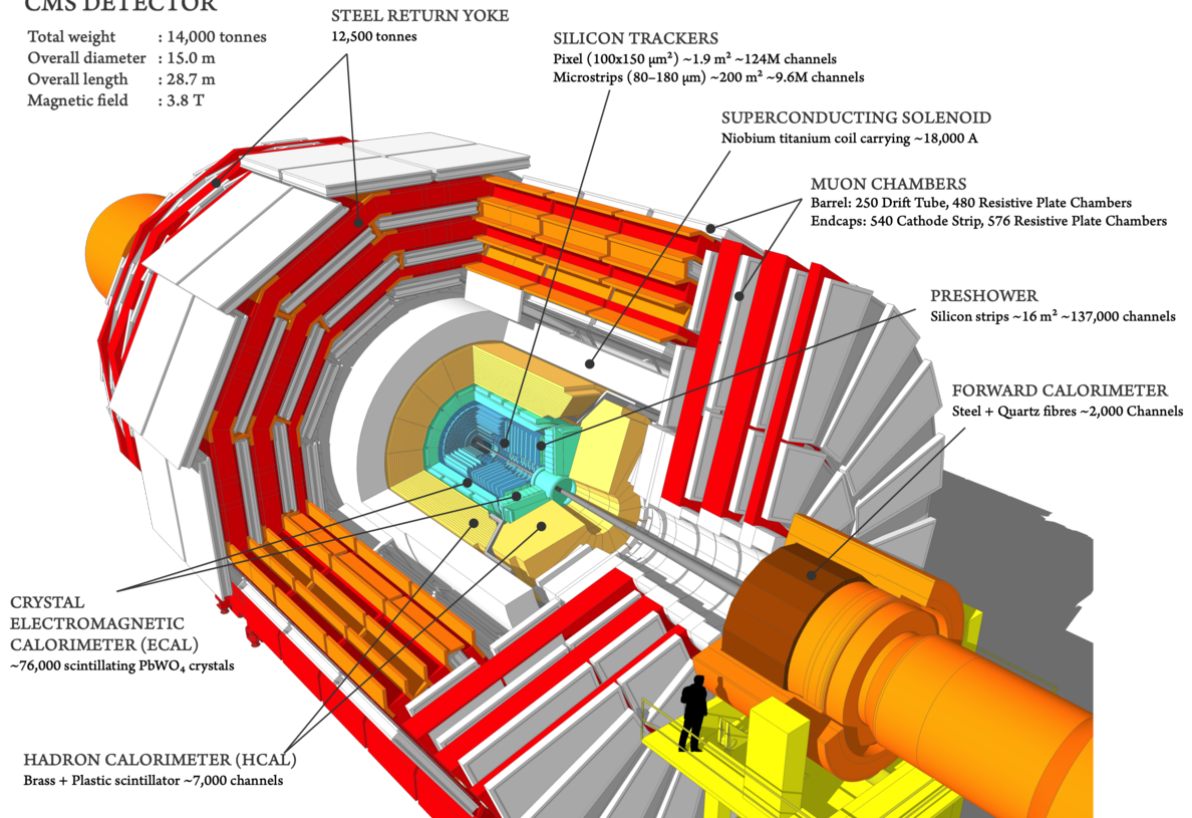


Figure 2.1: The Compact Muon Solenoid (CMS) Detector(credits: CERN)

### 2.1.2 CMS Detector Design

The CMS detector consists of the following main parts:

- The Tracking System
- The Electromagnetic Calorimeter
- The Hadronic Calorimeter
- The Magnet System
- The Muon Chambers

A cross-sectional view of the CMS detector, illustrating its different layers for the detection of various particles, is shown in Figure 2.2.

### 2.1.3 The Tracking System

As shown in Figure 2.7, the tracking system is the innermost sub detector system. Because it is next to the point where the beams interact, this is where the particle flux is at its highest. When building this system, particular consideration must be given to spatial resolution and its component's resilience to forceful collisions. The spatial resolution allows us to distinguish between various charged particles. To do this, three concentric layers of "Silicon Pixel Detectors," each measuring  $100 \times 150 \mu\text{m}^2$ , are arranged. It is possible to attain a spatial resolution of  $10 \mu\text{m}$  and  $20 \mu\text{m}$  in the  $z$ -direction and  $r\phi$ -plane, respectively, by employing specialty filter techniques.[5] Ten layers of "Silicon Strip Detectors" are positioned 20–110 cm from the beam intersection point. These detectors only provide 2D information about any hit due to the shape of the device. These layers are twisted in the direction of the third dimension.

Separated by  $110 \mu\text{rad}$ , their single point resolution in the  $r\phi$  direction and  $z$ -axis ranges from 23–52  $\mu\text{m}$  to 230–530  $\mu\text{m}$ , depending on the distance to the beam pipe.

respectively. Silicon strip detectors are much cheaper as compared to Silicon pixel detectors but in high particle flux, these detectors would show ambiguous results because of lack of third dimension. The central tracking system is capable of detecting any type of charged particle. A charged particle traveling through silicon ionizes the silicon atoms, causing a current to flow because the ionization process is enhanced by high voltage applied.

Charged particles are bent by a magnetic field. Particles in a detector are thus identified by their spiral arc. The particle's momentum is determined by the arc's curvature. We are able to precisely measure the impact parameters and the position of the secondary vertices thanks to the tracking detectors [3]. For the purpose of identifying jets produced by b-quarks (bottom quarks), impact parameters are crucial.

### 2.1.4 The Electromagnetic Calorimeter

A scintillation calorimeter is the electromagnetic calorimeter (ECAL) (see Figure 2.8) composed of lead tungstate. By producing electron-positron pairs and bremsstrahlung, the entering particles—photons and electrons—create a chain reaction of secondary particles. [6] within the crystal. The direct measurement of energy is the number of photons generated. of the particle incident. Due to their inability to sense high magnetic fields, silicon avalanche photodiodes are used to detect scintillation light in the barrel region. Because vacuum phototriodes can withstand high exposure, they are used in the endcap region.

Apart from that, photon pairs from  $\pi^0$  decays and energetic single photons are separated from each other using silicon detectors and pre-shower detectors, which are composed of lead absorbers, placed in front of endcaps. Crystals covering 10 with a length of 23 cm in the  $\theta$  and  $\phi$  directions result in a lead tungstate radiation length of 25.8. About 50% of the relative energy resolution is achieved by ECAL for electrons with transverse energy equal to 75 GeV.

### 2.1.5 The Hadronic Calorimeter

The Hadronic Calorimeter (HCAL), which consists of brass absorber material and plastic scintillators, is essentially a sampling calorimeter (see Figure 2.9). Hadron scattering produces a cascade of secondary particles through an inelastic process. A small portion

of the energy is utilised for detection in scintillator material, with the majority of the energy being deposited onto the material that absorbs it. For this reason, compared to ECAL, HCAL has coarser energy resolution. Fibres with variable wavelengths move the shimmering illumination. Fibres to hybrid photo diodes, which can function at high magnetic fields, are cleared by scintillation light. The calorimeter is also supported by additional detectors (outside magnetic coil) to improve the accuracy of high energetic jets. In summary, hadronic jets can be measured up to 11 hadronic interaction lengths away. The forward calorimeter measures the instantaneous luminosity and covers the pseudorapidity range

$$3.0 < |\eta| < 5.0$$

. Due to the high particle flux in the aforementioned pseudorapidity range, the calorimeter in this region is composed of steel absorbers with quartz fibres embedded in them. The calorimeter's miraculous coverage makes it possible to measure "Missing Transverse Energy" (ET) accurately. However, for incoming particles with the same energy, the response of HCAL and ECAL differs. Other than that, the calorimeter is not uniform over the entire pseudorapidity range. As a result, calibration is required for the sub detector's off set and scale in relation to pseudorapidity and transverse momentum. Specifics are available in [7].

### 2.1.6 The Magnet System

The magnet system serves as the focal point of the entire CMS experiment. In reality, the CMS detector's magnet is a "solenoid." It is made up of a "Superconducting Coil" that is used to pass electricity. Its diameter is 5.9 metres and its length is 13 metres.

without encountering any resistance and producing a magnetic field that is approximately 4.0 T, one million times more powerful than the earth's magnetic field. The world's largest magnetic system is this superconducting magnet system. It has a huge energy storage capacity because it can melt eighteen tonnes of gold.

This coil's primary function is to bend the incoming beam because it takes a very strong magnetic field to deflect a beam with this much energy. The system's primary parameters are the magnetic field's 4 T strength and the yoke's 14.

diameter between flats, an axial yoke with a length of 21.6 m, including endcaps, and a total weight of about 12,000 tonnes. Since the magnet can hold the inner trackers and calorimeters for

$$|\eta| < 1.5$$

, it can be thought of as the "supporting structure" for the detector's inner components.

### 2.1.7 The Muon Chambers

A "iron return yoke" is installed in the muons system (see Figure 2.10). Because muons are the least ionising particles, they can cross the iron while other particles cannot. Gaseous detectors are used in to provide a wide coverage area in

muon-filled space. Drift tubes (DT) made of aluminium are used in the barrel region. Cathode strip chambers (CSC), which can also function precisely in spatially variable B-fields, are installed in endcaps. DT and CSC provide spatial information needed to determine the precise value of muon momentum. Other than that, resistive plate chambers (RPC) are installed in the barrel and endcap region. RPCs can operate at high rates and provide quick information for Level-1 triggers.

In muon chambers, the detection efficiency for muons is greater than 98barrel region, there is only some percent momentum resolution [10]. By using combination of inner tracking system and muon chambers, the path of muons can be precisely determined

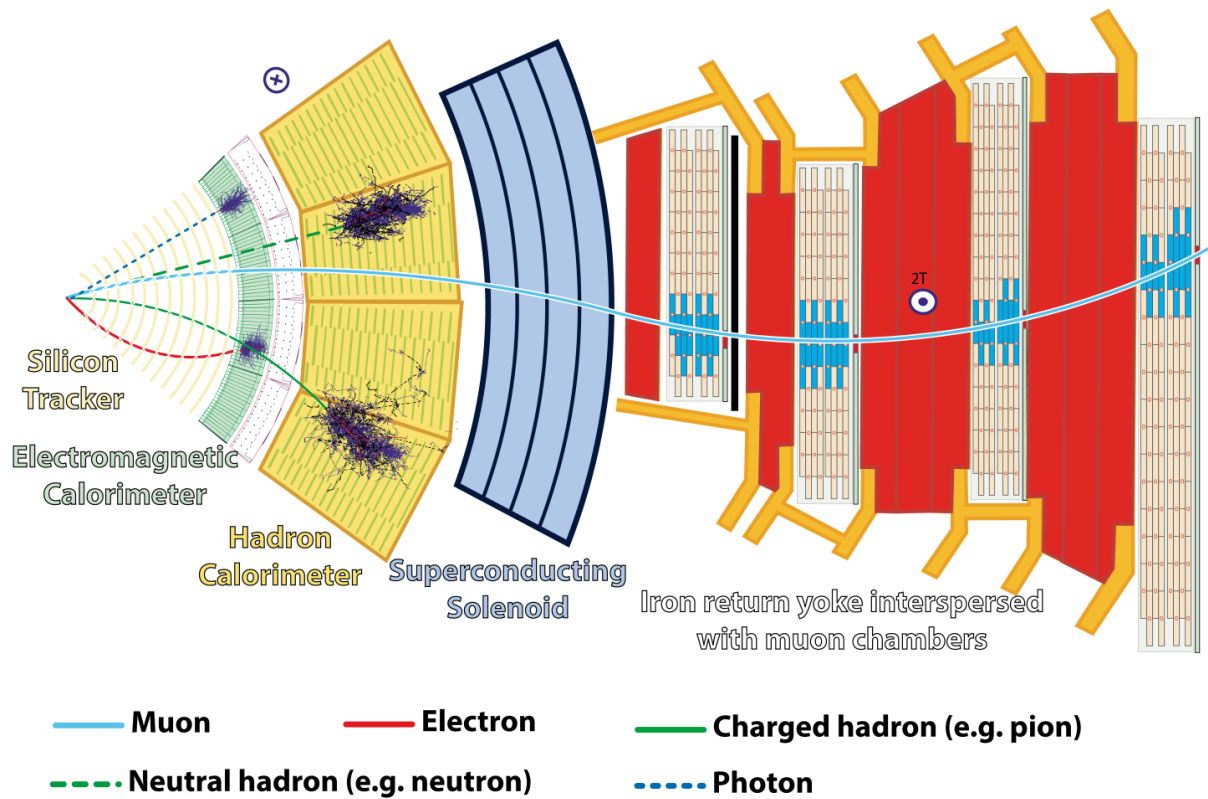


Figure 2.2: Components of the CMS Detector

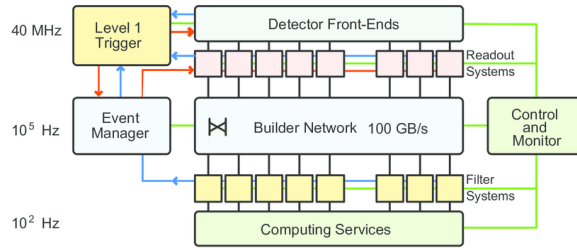


Figure 2.3: Data acquisition system of CMS experiment

## 2.2 Trigger and Data Acquisition System

Approximately one billion collisions at the intended luminosity occur in the CMS detector every second, but due to computing facility limitations, only a small portion of these events—roughly 400—can be recorded to disc for analysis. Therefore, in order to decrease the amount of data that can be readily stored on machines, we must apply some triggers. IT experts are working to enhance the computing facilities as well, and we have noticed a notable rise in computing power in recent months, particularly during the LHC machine’s shutdown following the 2008 incident.

Hardware is used to implement the Level-1 trigger. The data needed to choose a trigger is provided by the calorimeter and the muon system. Hardware buffers store the entire event data if a decision is made, and they flush that data out in the event that the Level-1 trigger fails. Thus, at a rate of about 100 kHz, events that pass the first step can be forwarded to the second trigger step. Programmes use High Level Trigger (HLT) implementation. Thus, algorithms that are the same or comparable to offline reconstruction can be used. Additionally, HLT can be reconfigured while it is in use.

Now This will help us to analyse the dimuons produced in the decay that are detected by CMS we will see how this analysis takes place in the following chapter.

## CHAPTER 3

# Dimuon Analysis in Particle Physics

Dimuon spectrum analysis is a pivotal technique in particle physics for studying muon pairs produced in high-energy collisions. This method has facilitated significant discoveries and advancements in the field, enhancing our understanding of the fundamental components and forces of the universe.

### 3.0.1 Introduction

Particle physics explores the fundamental particles of the universe and the forces governing their interactions. Dimuon spectrum analysis, involving the study of muon pairs from high-energy collisions, plays a crucial role in discovering and characterizing particles.

### 3.0.2 Particle Production in High-Energy Collisions

High-energy collisions, such as those in particle accelerators or from cosmic rays, produce a variety of particles, including muons. These muons are detectable in particle detectors due to their relatively long lifetimes compared to other subatomic particles.

### 3.0.3 Dimuon Production Mechanisms

Dimuons are produced through various processes:

- Hadron decays: Mesons and baryons decaying into muon pairs.
- Resonance decays: Heavy particles like the  $J/\psi$  and  $Y$  mesons decay into muon pairs, appearing as distinct peaks in the dimuon spectrum.
- Electroweak processes: These rare processes produce muon pairs through weak interactions.

### 3.0.4 Experimental Setup and Data Analysis

Particle detectors equipped to detect muons measure their trajectories, energies, and momenta. Data analysis techniques are employed to reconstruct the dimuon spectrum and extract key information such as resonance masses and decay properties.

### 3.0.5 Discovery and Characterization of New Particles

Dimuon spectrum analysis has led to significant discoveries:

- Charmonium and bottomonium states confirming the existence of charm and bottom quarks.
- Potential new physics phenomena indicated by deviations from Standard Model predictions.

### 3.1 Indirect detection of particles

Particles cannot always be directly detected, as previously mentioned with the CMS or other particle detectors. Many intriguing processes have short lifespans, necessitating their detection through indirect means. As previously stated, it is not always possible to directly detect particles, as is the case with the CMS or other particle detectors. Some interesting processes have brief lifespans, which requires them to be located within longer-lasting processes. As a result, the detection of these particles is an indirect process.

As an example let us take The decay of the Z boson can occur in 24 different ways. Within this exercise, only one of these decay processes is detected: when the Z boson decays into a muon and an antimuon. An illustration of this decay process is depicted as a Feynman diagram in Figure[8]

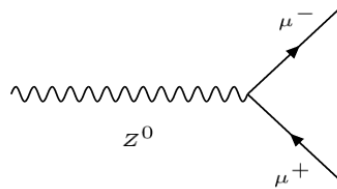


Figure 3.1: The process where the Z boson decays to the muon and the antimuon

Muons created in the decay process can be detected with the CMS. However, detecting only the muon and the antimuon is not sufficient evidence for the existence of the Z boson. The detected two muons could originate from any of the processes occurring in the collision event (since many different processes occur simultaneously). Therefore, the mass of the Z boson must also be reconstructed.

#### The invariant mass

The mass of the particles can be determined with the help of a concept called invariant mass. Let's derive an expression for the invariant mass.

Consider a situation where a particle with mass  $M$  and energy  $E$  decays into two particles with masses  $m_1$  and  $m_2$ , and energies  $E_1$  and  $E_2$ . Conservation of energy and momentum holds in the decay process, so  $E = E_1 + E_2$  and  $\vec{P} = \vec{P}_1 + \vec{P}_2$ .

Particles obey the relativistic dispersion relation:

Particles will obey the relativistic dispersion relation:

$$Mc^2 = \sqrt{E^2 - c^2\vec{p}^2}.$$

And with the conservation of energy and momentum, this can be shown as[8]

$$Mc^2 = \sqrt{(E_1 + E_2)^2 - c^2(\vec{p}_1 + \vec{p}_2)^2}$$

$$\begin{aligned}
&= \sqrt{E_1^2 + 2E_1E_2 + E_2^2 - c^2\vec{p}_1^2 - 2c^2\vec{p}_1 \cdot \vec{p}_2 - c^2\vec{p}_2^2} \\
&= \sqrt{2E_1E_2 - 2c^2|\vec{p}_1||\vec{p}_2|\cos(\theta) + m_1^2c^4 + m_2^2c^4}. \quad (1)
\end{aligned}$$

The relativistic dispersion relation can be expressed in the following format

$$M^2c^4 = E^2 - c^2\vec{p}^2$$

$$E = \sqrt{c^2\vec{p}^2 + M^2c^4},$$

from where by setting  $c = 1$  (very common in particle physics) and by assuming masses of the particles are very small compared to momenta, it is possible to derive

$$E = \sqrt{\vec{p}^2 + M^2} = |\vec{p}| \sqrt{1 + \frac{M^2}{\vec{p}^2}} \xrightarrow{M \ll |\vec{p}|} |\vec{p}|.$$

By applying the result  $E = |\vec{p}|$  derived above and setting  $c = 1$  in equation (1), it can be reduced to the format

$$M = \sqrt{2E_1E_2(1 - \cos(\theta))},$$

where  $\theta$  is the angle between the momentum vectors of the particles. With this equation, it is possible to calculate the invariant mass for the particle pair if the energies of the particles and the angle  $\theta$  are known.

In experimental particle physics, the equation for the invariant mass is often in the form

$$M = \sqrt{2p_{T1}p_{T2}(\cosh(\eta_1 - \eta_2) - \cos(\phi_1 - \phi_2))}, \quad (2)$$

where transverse momentum  $p_T$  is the component of the momentum of the particle that is perpendicular to the particle beam,  $\eta$  is the pseudorapidity, and  $\phi$  is the azimuth angle. The pseudorapidity is defined using  $\theta$  with the equation  $\eta = -\ln(\tan(\frac{\theta}{2}))$ . Thus, pseudorapidity  $\eta$  essentially describes an angle. Similarly,  $\phi$  also describes an angle.

Image 8 expresses  $\theta$ ,  $\eta$ , and  $\phi$  in the CMS detector. The particle beams travel along the z-direction. Image 8 also illustrates that  $\eta$  approaches 0 when  $\theta = 90^\circ$  and approaches  $\infty$  when  $\theta = 0^\circ$ . [8]

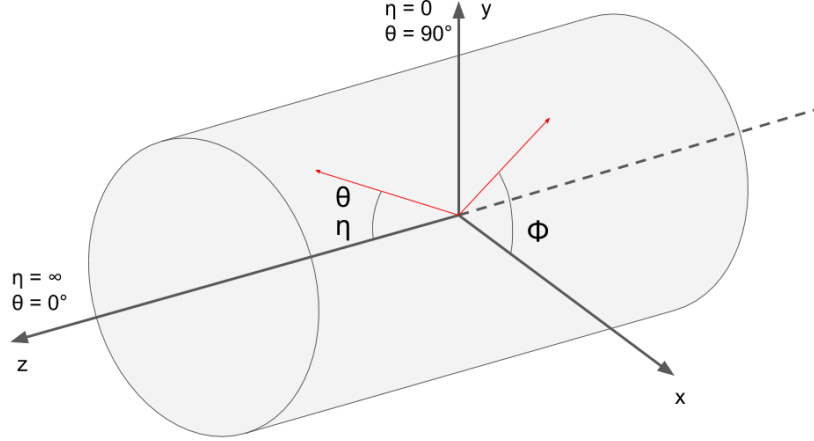


Figure 3.2: Quantities  $\eta$ ,  $\theta$ , and  $\phi$  in the CMS detector

## Reconstructing the particles Mass

To verify the existence of the Z boson, we analyze collision data where two muons are detected alongside other particles. The invariant mass of the muon pair in each collision event is calculated using Equation (2):

$$M = \sqrt{2p_{T1}p_{T2} (\cosh(\eta_1 - \eta_2) - \cos(\phi_1 - \phi_2))}$$

This calculation is repeated for a large number of collision events. If the calculated invariant mass matches the known mass of the Z boson, it indicates that the muon pair originates from the decay of a Z boson. Conversely, if the invariant mass differs significantly, the muons likely arise from different events.

Therefore, the invariant mass serves as compelling evidence for confirming the presence of the Z boson in particle collisions, distinguishing its decay from other observed particle interactions. Its the same with the remaining resonances. Here is the way on how we identify the particles.

## Identifying the particles

In practice, identifying the particles involves the following steps:

1. **Invariant Mass Calculation:** Calculate the invariant mass for pairs of muons from a large number of collision events using Equation (2):

$$M = \sqrt{2p_{T1}p_{T2} (\cosh(\eta_1 - \eta_2) - \cos(\phi_1 - \phi_2))}$$

2. **Histogram Creation:** Construct a histogram from the calculated invariant mass values. Each bin in the histogram represents a range of invariant masses, showing how many events fall into each range.
3. **Peak Identification:** Look for peaks in the histogram where many invariant mass values cluster together. A peak indicates that there were collisions where particles had an invariant mass corresponding to the peak value.

4. **Parameter Fitting:** Fit a suitable function (often a Gaussian function) to the histogram. The parameters of the fitted function, such as the mean (mass of the Z boson) and the width (related to the lifetime), provide precise measurements of the Z boson's properties.

This process allows physicists to identify the particles by studying the distribution of invariant masses from collision data. Peaks in the histogram confirm the presence of particles with masses corresponding to the particles. Fitting a function to the histogram refines the measurement, yielding accurate values for the particles mass and lifetime. All these analysis is done using software called ROOT.

## 3.2 ROOT for Analysis

ROOT (Reflective Object-Oriented Technology) is a powerful software framework developed at CERN, the European Organization for Nuclear Research, located in Geneva, Switzerland. Initially created to meet the demanding data analysis needs of particle physics experiments, ROOT has evolved into a versatile tool widely used across various scientific disciplines.

### Foundation and Evolution

ROOT was conceived in the late 1990s as a response to the escalating demands for processing and analyzing the vast amounts of data generated by experiments at CERN's Large Hadron Collider (LHC) and other high-energy physics facilities. Developed by a team led by Rene Brun and Fons Rademakers, ROOT was designed to optimize data storage, access, and visualization while maintaining robustness and efficiency.

Over the years, ROOT has undergone significant enhancements and expansions. It has grown from a data analysis tool into a comprehensive framework that supports simulation, statistical analysis, visualization, and more. Its development has been driven not only by the needs of particle physics but also by contributions from a global community of scientists and developers who use ROOT in diverse fields of research.

### Key Features and Capabilities

#### Data Handling and Storage

At its core, ROOT excels in efficient data handling. It employs a binary storage format within ROOT files, ensuring compactness and fast access to complex data structures. This capability is crucial for managing the petabytes of data generated by experiments such as those conducted at the LHC.

#### Visualization and Analysis

ROOT provides extensive visualization tools tailored for scientific data. It supports high-quality 2D and 3D graphics, histograms, statistical plots, and interactive visualizations. These tools enable researchers to explore data intuitively, identify patterns, and present findings effectively.

## Mathematical and Statistical Libraries

ROOT integrates powerful libraries for numerical computation, statistical analysis, and mathematical modeling. These libraries include algorithms for data fitting, optimization, and simulation, empowering researchers to extract meaningful insights from complex datasets.

## Data Structures and Performance

Central to ROOT's efficiency is its use of advanced data structures like TTrees, optimized for storing and accessing large volumes of data with minimal memory footprint. This capability supports rapid data retrieval and manipulation, essential for real-time analysis and simulation in experimental physics.

## Interoperability and Extensibility

ROOT interfaces seamlessly with other programming languages, notably C++ and Python, enhancing its versatility and usability in diverse scientific environments. Researchers can integrate ROOT with existing workflows, develop custom extensions, and leverage community-contributed modules to address specific research challenges.

## Applications Across Scientific Domains

While rooted in particle physics, ROOT has transcended its origins to become a foundational tool in numerous scientific disciplines. It is widely used in astronomy, biology, geophysics, and other fields that rely on complex data analysis and simulation. ROOT's adaptability and robust performance make it indispensable for research projects ranging from studying the cosmos to understanding genetic sequences.

## Impact and Contributions to Science

ROOT has played a pivotal role in several landmark discoveries in particle physics, including the observation of the Higgs boson at the LHC in 2012. Its sophisticated data analysis capabilities have enabled researchers to sift through massive datasets, validate theoretical models, and uncover new physics phenomena. Beyond specific discoveries, ROOT's open-source nature and collaborative development model foster innovation and knowledge-sharing within the global scientific community.

ROOT CERN stands as a testament to the power of collaborative scientific innovation. From its inception at CERN to its widespread adoption across scientific disciplines worldwide, ROOT has revolutionized data analysis, visualization, and simulation capabilities. As scientific questions grow more complex and datasets larger, ROOT continues to evolve, ensuring that researchers have the tools they need to push the boundaries of human knowledge.

**Lorentz Vectors and Particle Physics:** ROOT provides robust support for Lorentz vectors, crucial for representing particle momenta and energies in high-energy physics simulations and analyses.

**Fitting Tools:** ROOT incorporates sophisticated fitting algorithms for accurately modeling experimental data. These tools are essential for extracting precise parameters of particle properties and phenomena.

**DataFrames:** ROOT introduces DataFrames, enabling intuitive manipulation and analysis of structured data. This feature facilitates complex queries and statistical operations, vital in exploring relationships within experimental datasets.

ROOT's versatility extends to visualization tools that aid in interpreting results, making it indispensable in the discovery and analysis of particles such as the Higgs boson. For installation instructions, detailed documentation, and further exploration of ROOT's capabilities, visit <https://root.cern/>. We use ROOT to perform the Dimuon analysis.

## CHAPTER 4

# The Dimuon Spectrum

At first we will create the entire dimuon mass reconstruction from 0.25 GeV to 300 GeV. This spectrum shows us the number of events vs dimuons mass which is reconstructed on x axis this spectrum shows the resonances and these resonances corresponds to the particles from eta to z boson. Now from this we will take each resonance separately and fit those resonance with different fitting functions such as Gauss, crystal ball, BW distribution etc., but we need to use a background function to account for the offset in the resonance. The resonance before Z boson is not a particle but the trigger used.

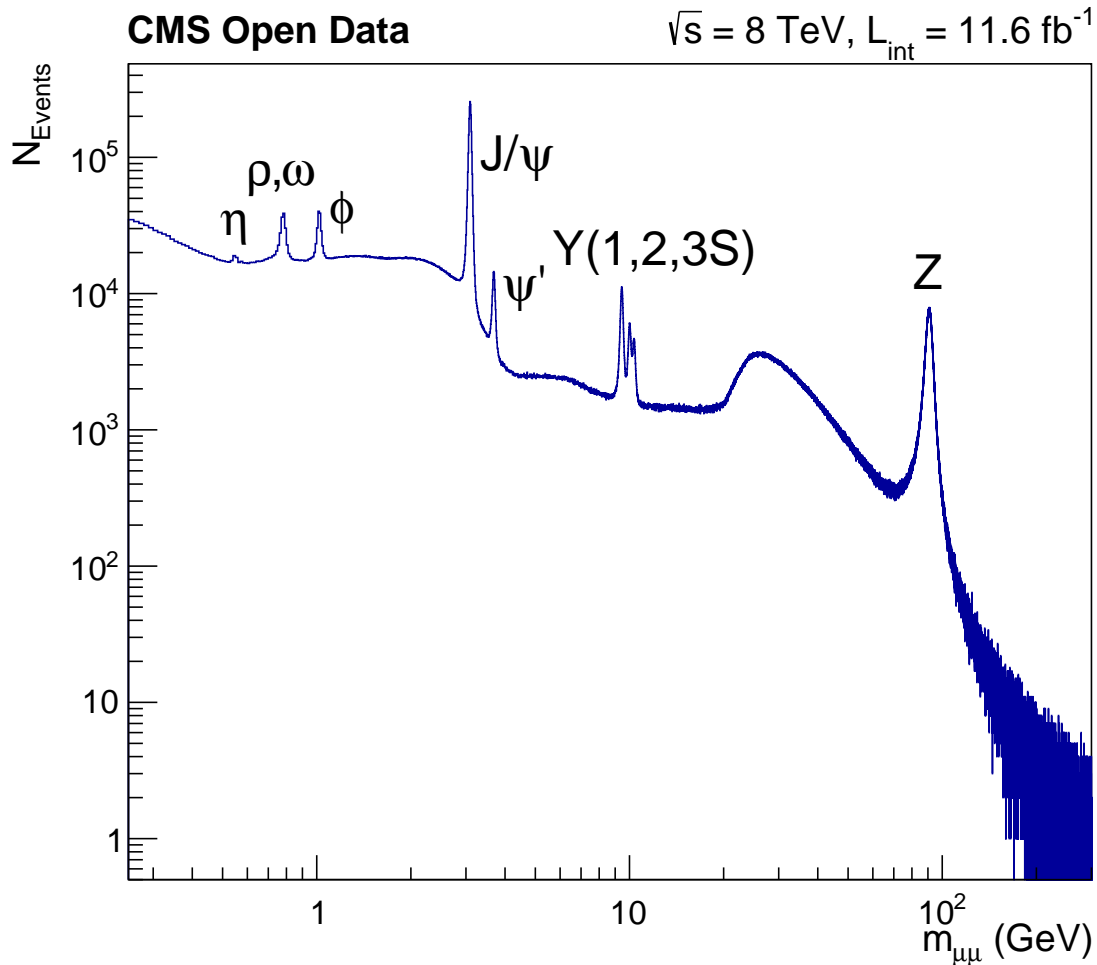


Figure 4.1: Dimuon spectrum

These resonances are fit with any of these fit functions discussed above to obtain the mass of each particle in the resonance and is compared to PDG live a repository for particle's data.

Now we will see how we can fit the all particle resonances. One easy way is to fit the resonances with the root fit panel by choosing the mass window close to the peak to resonance. The easy fit function we an use is the Gaussian function and with exponential background the fit is good when we are close to the peak resonance mass window. We can use different fit functions based on which will result in good fit to the particles resonance.

## 4.1 Meson Resonance Fits

### 4.1.1 Eta Particle $\eta$ Resonance Fit

The eta ( $\eta$ ) is an isosinglet mesons made of a mixture of up, down, and strange quarks and their antiquarks. The charmed eta meson ( $\eta_c$ ) and bottom eta meson ( $\eta_b$ ) are similar forms of quarkonium; they have the same spin and parity as the (light)  $\eta$  defined, but are made of charm quarks and bottom quarks respectively. The top quark is too heavy to form a similar meson, due to its very fast decay. The eta was discovered in pion–nucleon collisions at the Bevatron in 1961 by Aihud Pevsner et al. at a time when the proposal of the Eightfold Way was leading to predictions and discoveries of new particles from symmetry considerations.[14]

- Mass: Approximately  $547.862 \pm 0.018 \text{ MeV}/c^2$ .

We fit the eta resonance with a Gaussian function using a exponential background to obtain the mass of the particle:

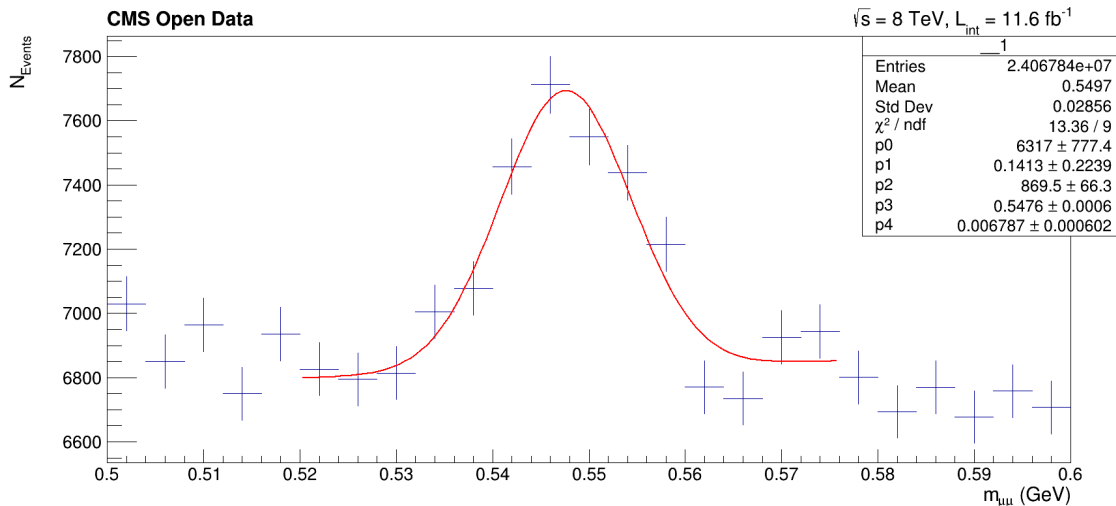


Figure 4.2: Eta Resonance Fit

In this figure, the parameter  $p3$  in the fitting gives the mass value of the eta particle.

- Mass: Approximately  $547.6 \pm 0.6 \text{ MeV}/c^2$ , which is close to the accepted value.

### 4.1.2 Omega Particle Resonance Fit

The superposition of an up quark-antiquark and a down quark antiquark pair produces the flavourless omega meson. Along with pions and rho mesons, it mediates the nuclear force and is a member of the vector meson nonet.[13]

- Mass: Approximately  $782.65 \text{ MeV}/c^2$ .

We fit it with a Voigt profile to obtain the mass of the particle:

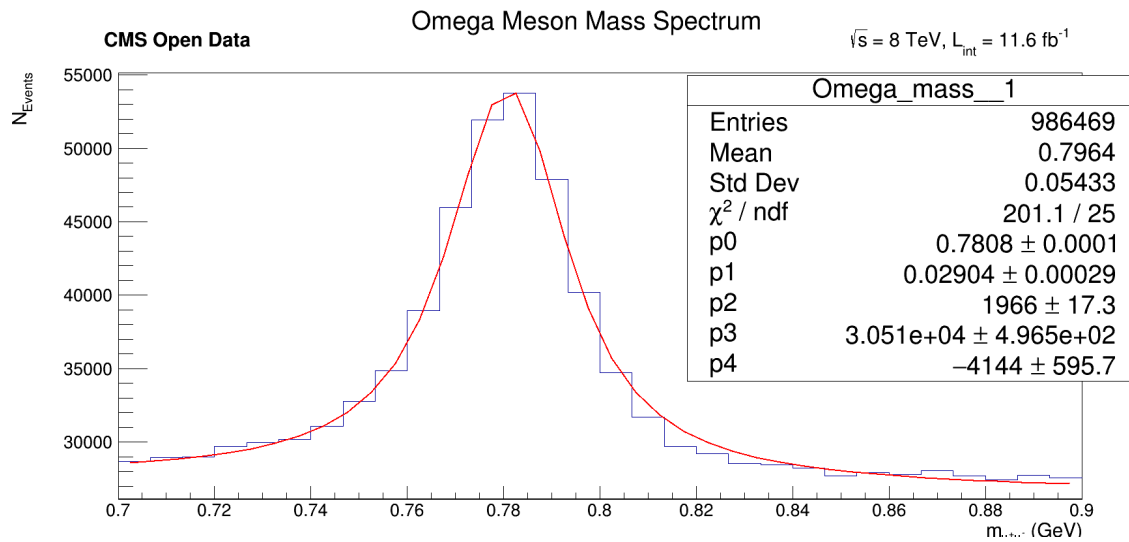


Figure 4.3: Omega Resonance Fit

In this figure, the parameter  $p0$  in the fitting gives the mass value of the omega meson.

- Mass: Approximately  $(780.8 \pm 0.1) \text{ MeV}/c^2$ , which is close to the accepted value.

### 4.1.3 Phi Particle $\phi$ Resonance Fit

Within particle physics, a strange quark and a strange antiquark combine to form the phi meson, also known as the  $\phi$  meson. It was the  $\phi$  meson's peculiar tendency to decay into  $K^0$  and  $\bar{K}^0$  that made the OZI rule known. Its mean lifetime is  $1.55 \pm 0.01 \times 10^{-22}$  s, and its mass is  $1019.461 \pm 0.020$  MeV/c<sup>2</sup>.

J. J. Sakurai, a Japanese American particle physicist, first proposed the existence of the *phi* meson in 1962 as a resonance state between the  $K^0$  and the  $\bar{K}^0$ . Later in 1962, while studying  $K^-p^+$  collisions at about 2.23 GeV/c, P.L. Connolly et al. found it in a 20-inch hydrogen bubble chamber at the Alternating Gradient Synchrotron (AGS) in Brookhaven National Laboratory in Upton, NY. In order to collide with protons, a beam of  $K^-$ s had to be accelerated to high energies.

- Mass: Approximately  $1019.461 \pm 0.020$  MeV/c<sup>2</sup>.

We fit it with a voigt function to obtain the mass of the particle:

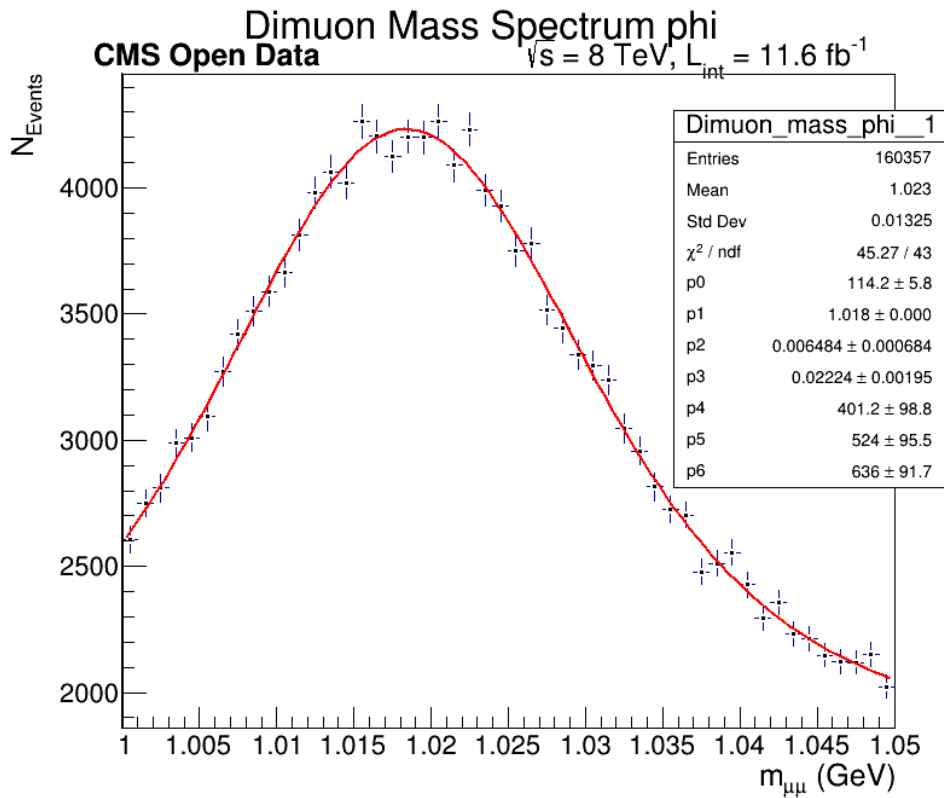


Figure 4.4: Phi Resonance Fit

In this figure, the parameter  $p1$  in the fitting gives the mass value of the phi particle.

- Mass: Approximately  $(1018 \pm 0)$  MeV/c<sup>2</sup>, which is close to the accepted value.

#### 4.1.4 J/Psi Particle $J/\psi$ Resonance Fit

The  $J/\psi$  (J/psi) meson, also known as the charm quark and charm antiquark meson, is a flavor-neutral subatomic particle. Mesons called "charmonium" or psions are typically formed by a bound state of a charm quark and a charm antiquark. Because of its low rest mass and spin of 1, charmonium is most commonly found in the form  $J/\psi$ . With a mean lifetime of  $7.2 \times 10^{-21}$  s, the  $J/\psi$  has a rest mass of  $3.0969 \text{ GeV}/c^2$ , slightly higher than the  $\eta_c$  ( $2.9836 \text{ GeV}/c^2$ ). This lifetime exceeded expectations by a factor of a thousand.[15]

Two research groups, led independently by Samuel Ting of MIT and Burton Richter of the Stanford Linear Accelerator Centre and Brookhaven National Laboratory, respectively, made the discovery. On November 11, 1974, they both announced their discoveries after realising they had discovered the same particle. The fact that the swift changes in high-energy physics that followed at the time are now collectively referred to as the "November Revolution" emphasises the significance of this discovery[citation needed]. In 1976, Richter and Ting received the Nobel Prize in Physics.[4]

- Mass: Approximately  $3097 \text{ MeV}/c^2$ .

We fit it with a Gaussian function to obtain the mass of the particle:

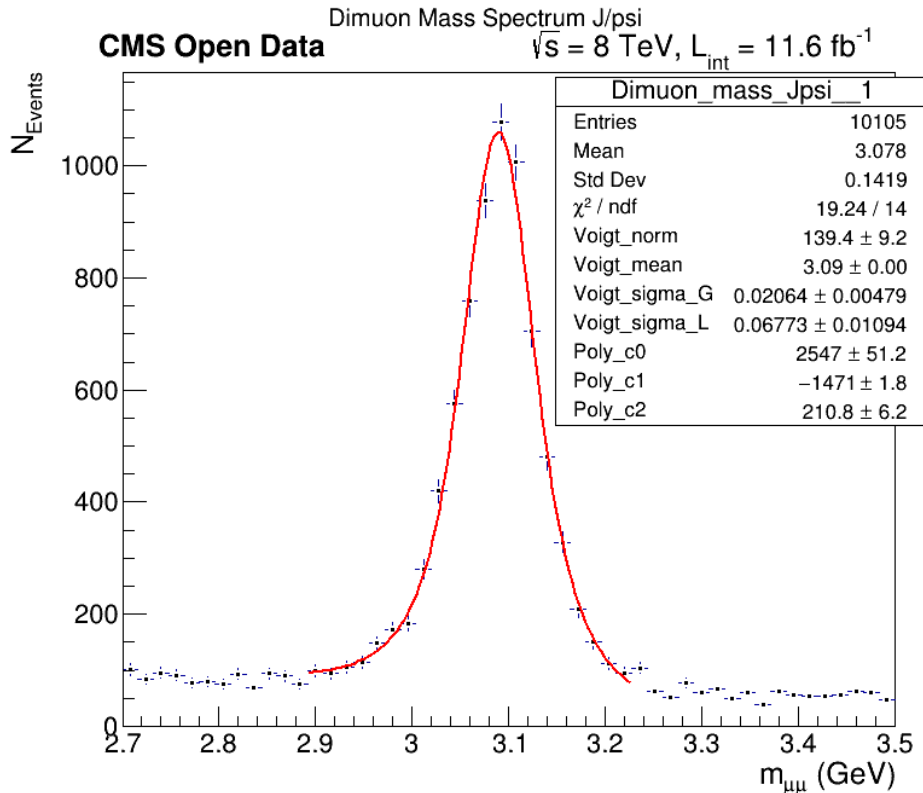


Figure 4.5: J/Psi Resonance Fit

In this figure, the parameter *voigtmean* in the fitting gives the mass value of the  $J/\psi$  particle.

- Mass: Approximately  $(3.09 \pm 0) \text{ GeV}/c^2$ , which is close to the accepted value.

### 4.1.5 Psi Prime $\psi'$ Resonance Fit

In the meantime during the  $J/\psi$  discovery, Richter's group discovered another resonant state with a slightly higher mass, which was called  $\psi'$ . The confirmation was so fast that it was actually published in the same issue of Physical Review Letters, i.e., vol. 33, no. 23, issued the second of December 1974. It was promptly established that the quantum numbers of the  $J/\psi$  were the same as those of the photon.[9]

The  $\psi'$  particle is an excited state of the  $J/\psi$  meson. It decays to dimuon in the final state and is detected in detectors.

- Mass: Approximately  $3686 \text{ MeV}/c^2$ .

We fit it with a voigt and a polynomial background to obtain the mass of the particle:

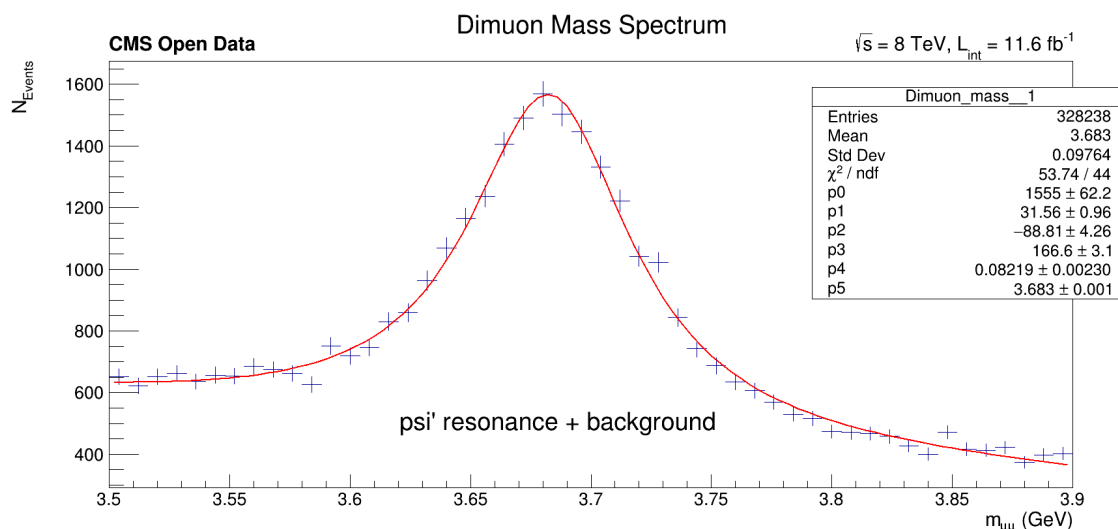


Figure 4.6: Psi Prime Resonance Fit

In this figure, the parameter  $p5$  in the fitting gives the mass value of the  $\psi'$  particle.

- Mass: Approximately  $(3.683 \pm 0.001) \text{ GeV}/c^2$ , which is close to the accepted value.

#### 4.1.6 Upsilon $Y(1S)$ Resonance Fit

Discovered in 1977 at Fermilab, the Upsilon meson, with a mass of  $9.46 \text{ GeV}/c^2$ , confirmed the existence of the bottom quark (b). Detected via electron-positron annihilation, its resonance validated the quark model's predictions and remains crucial in understanding particle interactions today.

The Upsilon particles  $Y(1S)$  are bottomonium states, composed of a bottom quark and an antiquark. They decay to dimuon in the final state and are detected in detectors.

- Mass: Around  $9460 \text{ MeV}/c^2$  (for  $Y(1S)$ ).

We fit it with a Voigt function to obtain the mass of the particle:

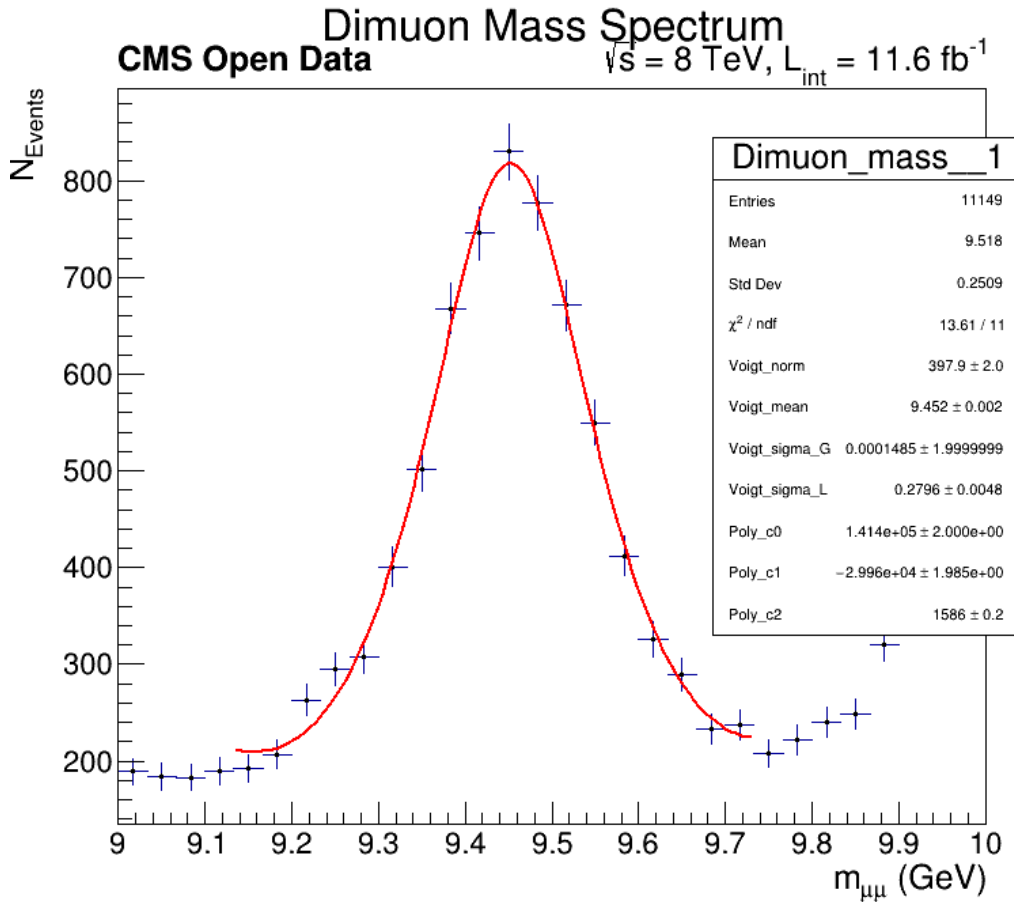


Figure 4.7: Upsilon Resonance Fit

In this figure, the parameter  $p3$  in the fitting gives the mass value of the Upsilon particles.

- Mass: Approximately  $(9.452 \pm 0.002) \text{ GeV}/c^2$ , which is close to the accepted value.

### 4.1.7 Z Boson Resonance Fit

Discovered in 1983 at CERN's Super Proton Synchrotron (SPS), the Z boson, with a mass around  $91.2 \text{ GeV}/c^2$ , confirmed the electroweak theory. Detected through electron-positron collisions, its identification provided key evidence for the unified theory of electromagnetic and weak forces, furthering our understanding of fundamental particle interactions.

The Z boson is a neutral gauge boson that mediates the weak nuclear force. It decays to dimuon pairs and is detected in detectors.

- Mass: Approximately  $91 \text{ GeV}/c^2$ .

We fit it with a Gaussian function to obtain the mass of the particle:

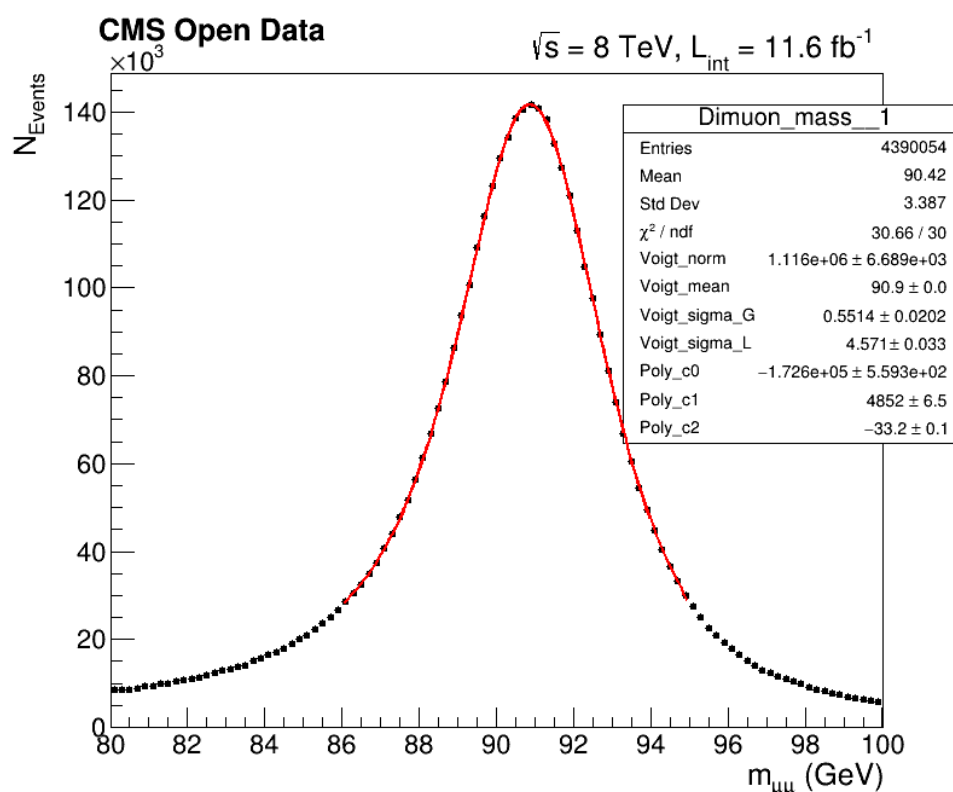


Figure 4.8: Z Boson Resonance Fit

In this figure, the parameter Voigt mean in the fitting gives the mass value of the Z boson.

- Mass: Approximately  $(90.9 \pm 0) \text{ GeV}/c^2$ , which is close to the accepted value.

until Now we did the analysis of resonance peaks by fitting them and obtaining mass, Now I proceed to the kinematics of some of these particles to get a nice overview of how the dimuons are detected in the cms with what properties which will help in better understanding of the analysis.

## CHAPTER 5

# Kinematics

The basic picture of a collision at the 13 TeV LHC is as follows. The two protons come in with back-to-back momenta of 6.5 TeV each, conventionally taken to be in the  $z$  direction. The proton mass is negligible compared to these energies, so we write the proton momenta as:

$$P_1^\mu = (6.5 \text{ TeV}, 0, 0, 6.5 \text{ TeV})$$
$$P_2^\mu = (6.5 \text{ TeV}, 0, 0, -6.5 \text{ TeV})$$

I like to think of the proton as a big vegetable soup. Most of the soup is broth (the soft gluons), but there are also chunks of potatoes or carrots in it (harder gluons, quarks, or antiquarks). If you collided two beams of soup against each other, most of the time, the broth would just scatter, making a big mess (minimum bias events). But sometimes, a potato will hit against a carrot (hard  $qg$  scattering) and you might get a significant amount of splatter going in transverse directions to the beams. It is these collisions we are most interested in.

When there is a hard scatter, we write the parton momenta as:

$$p_1^\mu = x_1 P_1^\mu$$
$$p_2^\mu = x_2 P_2^\mu$$

Here,  $x_1$  and  $x_2$  are the fraction of the protons' momenta in the scattering partons. According to the parton model,  $x_1$  and  $x_2$  are distributed probabilistically and independently. That is, the probability of finding momentum fraction  $x_1$  in proton one is independent of what happens in proton two. This independence is an example of factorization, key to being able to calculate anything at all at the LHC using perturbation theory.[11]

Now, we have these partons of momenta  $p_1^\mu$  and  $p_2^\mu$  colliding at very high energy. Say they collide to produce a  $Z$  boson, which then decays into an  $e^+e^-$  pair. We might be interested in the angular separation between these leptons. We can measure the azimuthal angle  $\phi$ , around the cylinder described by the beamline, and also the polar angle  $\theta$ , defined with the beams at  $\theta = 0$  and  $\theta = \pi$ , and the center of the beams at  $\theta = \frac{\pi}{2}$ , as in the figure.

If  $(p_1^\mu + p_2^\mu)^2 = m_Z^2$ , the  $Z$  is produced at rest in the partonic center-of-mass frame. However, in the lab frame, the  $Z$  is not at rest because  $p_1^\mu + p_2^\mu$  can have some net  $z$ -momentum,  $p_z$ . Thus, the  $e^+e^-$  pair will be back-to-back in azimuth ( $\Delta\phi = \pi$ ), however, their separation in  $\theta$  will depend on this net  $p_z$ . If  $p_z = 0$ , the leptons will have equal and opposite polar angles. But if the pair has some net momentum along the  $z$ -axis, they will get closer together in  $\theta$ . [11]

To see this most clearly, consider very large  $p_z$  where both leptons are close to  $\theta = 0$ . In fact, values and differences of angles tend to tell us more about the parton momenta in the proton than about the angular distribution from Z decays.

Because angles in the lab frame are generally not very interesting from the point of view of the partonic collision, we like to work with variables which have the same values in the lab and partonic center-of-mass frame. Such variables are longitudinally boost invariant. A Lorentz boost along the  $z$ -direction can be parameterized by a number  $\beta$  as:

$$K_z = \begin{pmatrix} \cosh \beta & 0 & 0 & \sinh \beta \\ 0 & 1 & 0 & 0 \\ 0 & 0 & 1 & 0 \\ \sinh \beta & 0 & 0 & \cosh \beta \end{pmatrix}$$

A generic momentum  $p^\mu = (E, p_x, p_y, p_z)$  transforms under  $p^\mu \rightarrow K_z \cdot p$  as:

$$E \rightarrow E \cosh \beta + p_z \sinh \beta$$

$$p_x \rightarrow p_x$$

$$p_y \rightarrow p_y$$

$$p_z \rightarrow p_z \cosh \beta + E \sinh \beta$$

Thus, the  $x$  and  $y$  components of the momentum,  $p_x$  and  $p_y$ , called the transverse momenta, are boost invariant. We often use both the vector and scalar transverse momentum:

$$\mathbf{p}_T = (p_x, p_y), \quad p_T = |\mathbf{p}_T|$$

The azimuthal angle  $\phi$  is given by:

$$\phi = \tan^{-1} \left( \frac{p_y}{p_x} \right)$$

which is also boost invariant.

To find another boost invariant quantity, let us introduce the shorthand  $c = \cosh \beta$  and  $s = \sinh \beta$  so that  $c^2 - s^2 = 1$ . Then, under a boost:

$$\frac{E + p_z}{E - p_z} \rightarrow \left\{ \frac{E(c + s) + p_z(c + s)}{E(c - s) - p_z(c - s)} \cdot \frac{c + s}{c - s} \right\} = \left( \frac{E + p_z}{E - p_z} \right) (c + s)^2$$

That is, under a boost, this combination rescales by a  $z$ -dependent but momentum-independent amount. The log of this combination therefore shifts under a boost and the difference of logs is independent of  $\beta$ . This motivates defining rapidity as:

$$y = \frac{1}{2} \ln \left( \frac{E + p_z}{E - p_z} \right)$$

Under a boost:

$$y \rightarrow y + \ln(c + s)$$

The difference of rapidities  $y_1$  and  $y_2$  for two momenta  $q_1$  and  $q_2$  is boost invariant. We therefore define the angular separation as:

$$\Delta R = \sqrt{(\Delta \phi)^2 + (\Delta y)^2}$$

This angular separation is boost invariant. Plotting distributions as functions of rapidity rather than polar angle makes it easier to disentangle the physics of the protons that produced the boost from the physics of the hard collision that we are studying.

To get intuition for rapidity, consider massless particles. These have  $E = p$ . Then, drawing a little momentum triangle:

$$\cos \theta = \frac{p_z}{p} = \frac{p_z}{E}$$

So,

$$y = \frac{1}{2} \ln \left( \frac{E + p_z}{E - p_z} \right) = \frac{1}{2} \ln \left( \frac{1 + \cos \theta}{1 - \cos \theta} \right) = \frac{1}{2} \ln \left( \frac{2 \cos^2 \frac{\theta}{2}}{2 \sin^2 \frac{\theta}{2}} \right) = \ln \cot \frac{\theta}{2}$$

Thus, there is a simple mapping between rapidity and angle for massless particles. This motivates defining pseudorapidity as:

$$\eta = \ln \cot \frac{\theta}{2}$$

Some values for  $\theta$  and  $\eta$  are shown in the figure. Note that particles at  $\eta \approx 5$  are practically down the beam line. The ATLAS and CMS detectors measure particles up to pseudorapidities of around 5.

In summary, rapidity is a kinematic quantity defined as:

$$y = \frac{1}{2} \ln \left( \frac{E + p_z}{E - p_z} \right)$$

Rapidity itself is not boost invariant, but differences in rapidity are boost invariant. Other boost invariant quantities are  $p_T = \sqrt{p_x^2 + p_y^2}$  and  $\phi = \tan^{-1} \left( \frac{p_y}{p_x} \right)$ . Pseudorapidity  $\eta = \ln \cot \frac{\theta}{2}$  is a geometric quantity. It is equal to rapidity only for massless particles. For massive particles, differences in pseudorapidities are not boost invariant.[11]

## 5.1 Coordinate Systems

In this context, we use a right-handed coordinate system. The positive  $z$ -axis is aligned along the beam in the direction of the protons, and the positive  $y$ -axis points up. We sometimes use cylindrical  $(r, \phi, z)$  coordinates, as well as spherical  $(r, \theta, \phi)$  coordinates. The angular variables are defined such that  $\theta = \pi/2$  is parallel to the positive  $y$ -axis, and  $\phi = 0$  is coincident with the positive  $z$ -axis.

Instead of  $\theta$ , it is often convenient to use the pseudorapidity  $\eta$  defined as:

$$\eta = - \ln \tan \left( \frac{\theta}{2} \right) \tag{5.1}$$

The pseudorapidity approximates the true rapidity,  $y$ , given by:

$$y = \frac{1}{2} \ln \left( \frac{E + p_z}{E - p_z} \right) \tag{5.2}$$

in the limit where  $m \ll E$  (where  $m$  is the invariant mass,  $m^2 = E^2 - p^2$ ).

It is also useful to use the transverse momentum, which is the momentum vector projected onto a plane perpendicular to the beam axis:

$$p_T = p \sin \theta \quad (5.3)$$

This is particularly useful because in a proton-proton (pp) collision, the momenta along the beam of the colliding partons are not known (since many of the products of the collision escape down the beam pipe). However, their transverse momenta are very small compared to their momenta along the beam, so one can apply momentum conservation in the transverse plane.

One can also define a transverse energy by:

$$E_T = E \sin \theta \quad (5.4)$$

When treated as a vector, the direction of  $E_T$  should be taken to be the same as the  $p_T$  vector.

## 5.2 Kinematic plots of the particle Resonances

From the PT (transverse momentum),  $\eta$  (pseudorapidity), and  $\phi$  (azimuthal angle) plots of dimuon events, we can gain a variety of insights about the kinematic properties and production mechanisms of different particle resonances. Here is what can be learned from each plot:

### Transverse Momentum (pT) Plot

#### Shape of the pT Distribution:

- The distribution's shape can indicate the energy and momentum transfer involved in the production of the particle resonance.
- For resonances like  $J/\psi$  or  $\psi'$ , a peak at lower PT values indicates they are produced with relatively low transverse momentum.
- Higher PT values may indicate the involvement of higher energy processes or particles originating from the decay of heavy quarks (like b-quarks for  $\Upsilon$  resonances).

#### Comparative Analysis:

- By comparing the PT distributions of different resonances (e.g.,  $J/\psi$  vs.  $\Upsilon$ ), differences in their production mechanisms and kinematic properties can be inferred.
- Variations in PT distributions can also highlight differences in the detector acceptance and efficiency for different particles.

### Pseudorapidity ( $\eta$ ) Plot

#### Production Angular Distribution:

- The  $\eta$  distribution reveals the angular spread of the dimuon events relative to the beam axis.
- A flat  $\eta$  distribution suggests isotropic production in the transverse plane, while more structured distributions can indicate specific production angles or detector effects.

### **Acceptance and Efficiency:**

- $\eta$  distributions can help identify regions of the detector with varying acceptance or efficiency, allowing for corrections in the analysis.

### **Comparative Analysis:**

- Comparing  $\eta$  distributions for different resonances can show how different particles are distributed in the detector and whether there are any systematic biases in the production or detection process.

### **Azimuthal Angle ( $\phi$ ) Plot**

#### **Uniformity Check:**

- Ideally, if there is no preferential production direction in the transverse plane, the  $\phi$  distribution should be uniform.
- Any deviations from uniformity might indicate azimuthal anisotropies or detector effects (such as gaps or inefficiencies in certain  $\phi$  regions).

#### **Symmetry and Correlations:**

- The  $\phi$  plot can be used to study symmetries and correlations in the production of particles.
- Azimuthal angle distributions are also useful for identifying potential biases in the detector setup.

#### **Comparative Analysis:**

- By comparing the  $\phi$  distributions of different resonances, consistency can be checked and any unexpected anisotropies that might suggest new physics or experimental issues can be identified.

### **Combined Insights**

#### **Kinematic Properties:**

- Together,  $PT$ ,  $\eta$ , and  $\phi$  distributions provide a comprehensive picture of the kinematic properties of the dimuon events.
- These plots help in understanding the production mechanisms, decay kinematics, and interaction dynamics of the resonances.

#### **Detector Performance:**

- Analyzing these distributions helps in assessing the performance and coverage of the detector.
- Identifying and correcting for regions with poor efficiency or acceptance improves the accuracy of the analysis.

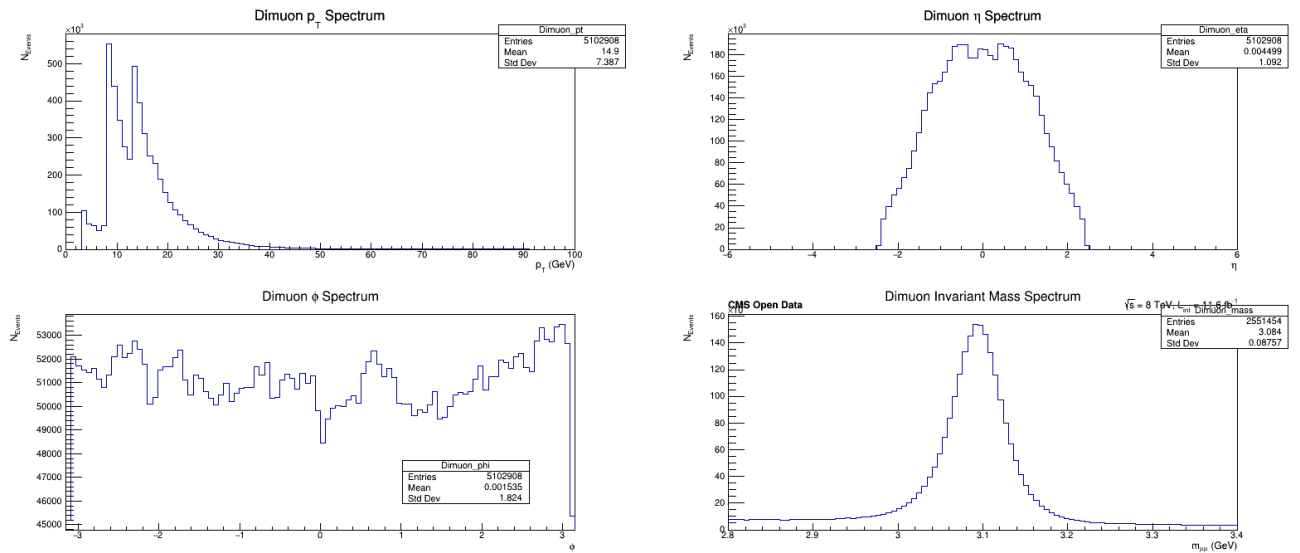


Figure 5.1: Kinematic plot of  $j/\psi$

### Physics Insights:

- Detailed study of these distributions can reveal underlying physics phenomena, such as differences in the production of resonances, potential new particles, or deviations from expected theoretical models.

These plots tell us how the muons kinematics were after the particle decays we can tell how the muons are behaving these will help us to build better detectors with good resolution.

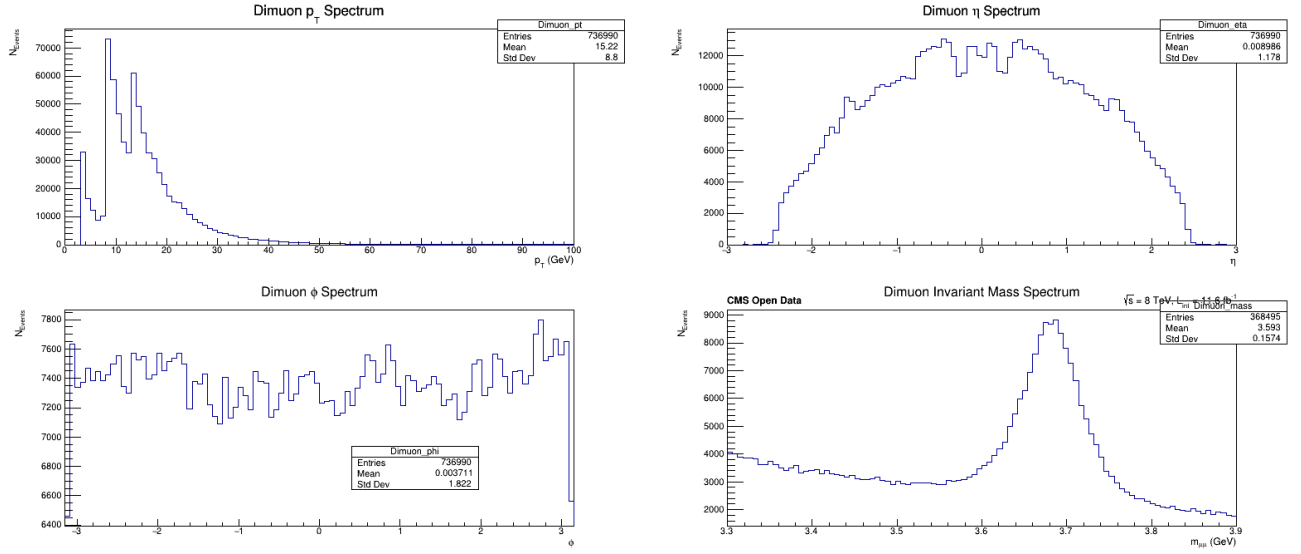


Figure 5.2: Kinematic plot of psi prime

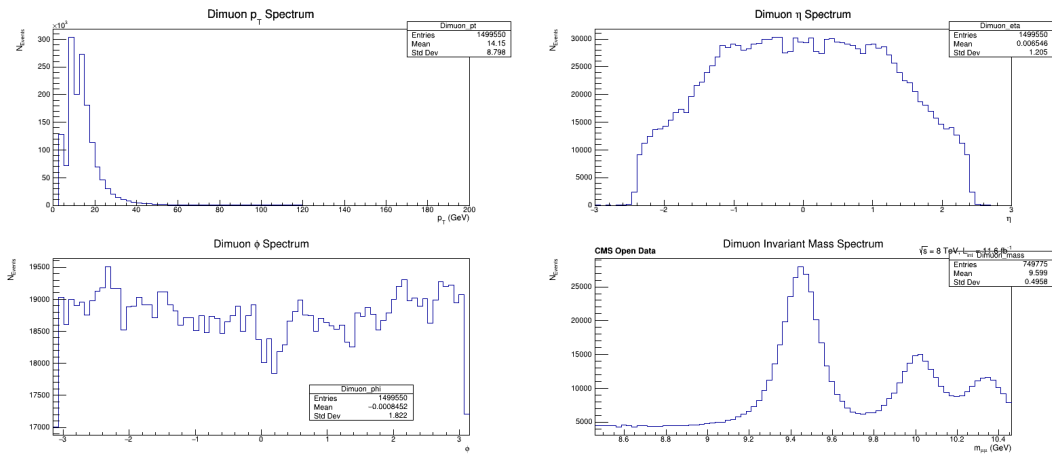


Figure 5.3: Kinematic plot of Upsilon

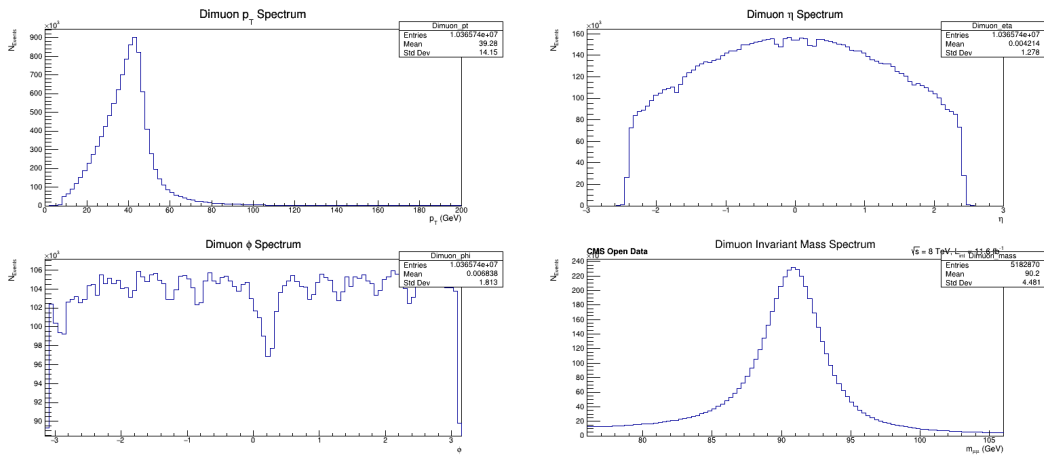


Figure 5.4: Kinematic plot of Z boson

## CHAPTER 6

# Conclusion and Future Work

‘In conclusion of this project the analysis of CMS open data using ROOT software, focusing on dimuon. We plotted the invariant mass spectrum for several particle resonances, including mesons and a Z boson. Using macros in ROOT, we fitted these resonances and obtained their invariant masses, comparing them with PDG live values. Additionally, we explored key kinematic variables such as transverse momentum, pseudorapidity, and azimuthal angle, which provide crucial insights into the nature of particles.’

The Standard Model (SM) of particle physics serves as a robust theoretical framework, explaining a wide array of natural phenomena. However, numerous experimental observations have emerged that challenge its completeness, prompting the development of various extensions. These extensions aim to address phenomena not accounted for by the SM.

The Large Hadron Collider (LHC), designed to explore both SM physics and potential new physics beyond it, commenced operations in 2009. Initially colliding proton beams at center-of-mass energies of 0.9 TeV and later 2.36 TeV, the LHC demonstrated remarkable machine and detector performance. In 2010, it achieved a center-of-mass energy of 7 TeV, a milestone in particle collider history, ushering in a new era of experimental high-energy physics research.

In 2012, the CMS (Compact Muon Solenoid) experiment at the LHC played a pivotal role. It confirmed the discovery of the Higgs boson, a cornerstone of the SM, through the analysis of proton-proton collisions. This discovery validated the Higgs mechanism and provided crucial insights into the origin of particle mass. The decay of the Higgs boson to dimuons is indeed an active area of investigation within the CMS experiment. Detecting and studying these rare decay events provides valuable insights into the properties of the Higgs boson, including its coupling strengths to different particles. By analyzing such decays, researchers can further refine our understanding of the Higgs mechanism and potentially uncover deviations from the predictions of the Standard Model, hinting at new physics phenomena.

Continued operation and upgrades of the LHC, including increased collision energies and enhanced detector capabilities, have enabled further exploration. These efforts seek not only to consolidate our understanding of the SM but also to probe potential new physics phenomena that lie beyond its current reach.

# References

- [1] Dark energy, dark matter. <http://science.nasa.gov/astrophysics/focus-areas/what-is-dark-energy/>. Accessed: 2024-07-05.
- [2] Grand unified theories. <http://pdg.lbl.gov/2010/reviews/rpp2010-rev-guts.pdf>. Accessed: 2024-07-05.
- [3] Impact parameter for nuclear scattering. <http://hyperphysics.phy-astr.gsu.edu/hbase/nuclear/impar.html>. Accessed: 2024-07-05.
- [4] Press release. <https://www.nobelprize.org/prizes/physics/1976/press-release/>, 2024. NobelPrize.org. Nobel Prize Outreach AB 2024. Fri. 5 Jul 2024.
- [5] Austin Ball, Michel Della Negra, L. Foà, and Achille Petrilli. Cms technical design report, volume ii: Physics performance. *J. Phys.*, G34:9951579, 2007.
- [6] Jill Bechtold. Bremsstrahlung. <http://boojum.as.arizona.edu/~jill/A300b/Lectures/Bremsstrahlung.pdf>. Accessed: 2024-07-05.
- [7] CMS Collaboration. Jet energy calibration and transverse momentum resolution in CMS. CMS Physics Analysis Summary CMS-PAS-JME-10-011, CMS, 2011.
- [8] CMS Open Data Education. CMS Open Data - Z Boson Exercise. <https://github.com/cms-opendata-education/zboson-exercise>, Year accessed.
- [9] JEAN-PHILIPPE LANSBERG.  $J/\psi$  and production at hadron colliders: A review. *International Journal of Modern Physics A*, 21(19n20):3857–3915, August 2006.
- [10] Michel Della Negra, L. Foà, A. Herve, and Achille Petrilli. CMS physics: Technical design report. Technical report, CERN, Geneva, 2006.
- [11] Matthew D. Schwartz. Tasi lectures on collider physics, 2017.
- [12] The Official String Theory Website. String theory. <http://www.superstringtheory.com/>. Accessed: 2024-07-05.
- [13] Wikipedia contributors. Omega meson — Wikipedia, the free encyclopedia, 2022. [Online; accessed 5-July-2024].
- [14] Wikipedia contributors. Eta and eta prime mesons — Wikipedia, the free encyclopedia, 2023. [Online; accessed 4-July-2024].
- [15] Wikipedia contributors.  $J/\psi$  meson — Wikipedia, the free encyclopedia, 2023. [Online; accessed 5-July-2024].

- [16] Wikipedia contributors. Large hadron collider — Wikipedia, the free encyclopedia, 2024. [Online; accessed 5-July-2024].
- [17] Worldwide LHC Computing Grid. Worldwide lhc computing grid (wlcg). <https://wlcg.web.cern.ch/>. Accessed: 2024-07-05.